www.ietdl.org

Published in IET Generation, Transmission & Distribution
Received on 3rd December 2011
Accepted on 23rd September 2012
doi: 10.1049/iet-gtd.2012.0340

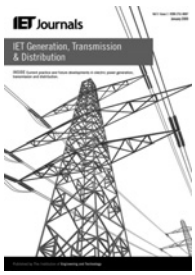

ISSN 1751-8687

Identification of generator loss-of-excitation from power-swing conditions using a fast pattern classification method

Eli Pajuelo, Ramakrishna Gokaraju, Mohindar S. Sachdev

Department of Electrical and Computer Engineering, University of Saskatchewan, 57 Campus Drive, Saskatoon, SK S7N 5A9, Canada
E-mail: rama.krishna@usask.ca

Abstract: This study describes a support vector machine (SVM)-based technique for identifying loss-of-excitation (LOE) condition in synchronous generators from other disturbances such as external faults and power-swing conditions. In this new approach, only one zone of LOE is required and the time coordination is reduced significantly. The proposed method is compared with traditional two-zone impedance method. Several operating conditions within the generator capability are used to verify the generality of the SVM-based classifier. The proposed classifier identifies an LOE condition in all cases before the impedance enters the larger mho impedance zone. Faults and power-swing conditions are identified correctly, thereby preventing incorrect operation of the LOE impedance zone.

1 Introduction

The loss-of-excitation (LOE) is a protection function that detects the failure of excitation to the field winding of synchronous generators [1, 2]. Losing the excitation means that the reactive power flow is reduced or even reversed, thus absorbing reactive power from the system. High-stator currents and end core heating are produced in the generator when this happens. The active power output also has a direct relationship with the field excitation when a large change happens such as those experienced during an LOE condition. The power transfer from rotor to stator is reduced because the magnetic coupling is weakened by the LOE condition and the generator may lose synchronism. Torque pulsation in the shaft and induced rotor currents are produced following a loss of synchronism. For the above reasons, an LOE condition may cause permanent damage to a generator.

The LOE protection is typically based on the apparent impedance measured at the output terminals of the generator. An LOE condition is detected when the impedance falls inside a predefined impedance zone for a specified amount of time. The most relevant work in this area dates back to 1949 when Mason [1] at General Electric introduced the use of a single-mho zone for the detection of LOE, and shortly after, Tremaine and Blackburn [2] at Westinghouse proposed a larger-mho zone which was limited by a directional element. The Mason approach was oriented more towards protection of severe LOE conditions whereas the Tremaine and Blackburn approach was intended to be more sensitive for alarm purposes. These approaches were quickly adopted by many utilities because of the improved selectivity compared to the DC current and voltage approach [3].

The impedance approach is not completely selective because other conditions may also activate it [4]. The conditions that sometimes fall inside the LOE impedance zone is the power-swing condition and some external fault conditions, thus creating a risk of incorrect operation. To prevent an incorrect operating decision, additional sophistication is required, such as the use of an additional impedance zone, and the use of time coordination, both proposed by Berdy [5] from General Electric in 1975. An alternative approach of combining time undervoltage in the AC and DC circuits was proposed by Lee *et al.* [6] while working at Ontario Hydro in 1979. Another approach of using admittance instead of impedance is described by Herrman and Smit [7] from Siemens. Tambay and Paithankar [8] proposed the use of rate of change of the apparent reactance instead of time coordination. Also, Li *et al.* [9] proposed the use of the δ angle between the internal voltage and the equivalent source for identification of LOE and loss of synchronism conditions. Usta *et al.* [10] proposed the use of pre-calculated levels of reactive power and time delays for the detection of LOE conditions. Yaghobi *et al.* [11] proposed the use of a search coil to detect the LOE by measuring the flux in the air gap of the machine. Shi *et al.* [12] provide a reasonable comparison between the most typical methods of detection of LOE conditions. Lee *et al.* [13] explain additional operational considerations to take to reduce the risk of incorrect LOE detection. Siwang *et al.* [14] provide a discussion to the current IEEE recommendations in the setting of traditional LOE impedance zone.

Application of modern digital techniques such as adaptive filtering techniques, pattern classification techniques, artificial neural networks (ANNs) and fuzzy logic to LOE protection has been very sparse in this area. In 1994, Sharaf and Lie [15] proposed a single-layered perceptron and a two-layer feed forward-based ANN for the identification of LOE and loss of synchronism conditions. The Sharaf and Lie classifier was based on the fast Fourier transform (FFT) of several synchronous machine variables such as the following: machine angle deviation, machine speed deviation, accelerating power deviation, output power, voltage, current and apparent admittance. From the FFT result, only a few dominant components were used to assemble the input vector for the classification. This classifier produced multiple outputs such as: fault or normal, first swing instability or LOE, allowable clearing time: long or short, type of LOE: short circuit or open circuit. The accuracy of this classifier ranged between 67 and 92%.

In 2007, So *et al.* [16] proposed an algorithm to identify power-swing conditions based on angular velocity and acceleration of the generator terminal voltage.

In 2009, Bo *et al.* [17] proposed an ANN-based method for the identification of LOE conditions. In this method the input features were: (a) excitation voltage applied, and (b) active power output. The accuracy of this classifier was of the order of 99%.

In 2010, Morais *et al.* [18] proposed a method based on the fuzzy inference mechanism. In his method, the input variables are apparent impedance and generator terminal voltage. A set of rules is defined based on known characteristic behaviour of these variables during an LOE condition. This method suggests and accuracy of 100% in the identification of an LOE from a power-swing condition.

In 2011, Bi *et al.* [19] proposed a method to dynamically modify the diameter of the mho LOE characteristic by using an estimate of the equivalent source impedance.

The support vector machine (SVM) method of pattern classification has been used by Seethalekshmi *et al.* [20]. In that paper, the SVM was used to classify between a real fault in the third impedance zone and other conditions such as power swing or voltage instability. Faults are typically faster disturbance when compared to the power swing or voltage instability cases, it should be noted.

In this paper, a new pattern classification method known as the support vector machine technique is proposed to identify a power swing from an actual LOE condition. This new method is simple and straightforward to apply and avoids the use of an additional impedance zone, directionality or undervoltage functions. One difference with Seethalekshmi *et al.* [20] work, is that here the power swing is a faster disturbance when compared with an LOE condition.

The SVM provides a method of separating two classes of data using non-linear mapping to higher dimension spaces. Generic mapping functions, such as Gaussian or polynomial functions, are typically used to obtain the separation between the classes. This kind of mapping is equivalent to producing a new feature by mathematical manipulation of the original data.

However, in this paper, a different approach is adopted by studying the behaviour of power and impedance curves during the various disturbances: LOE, faults and power swings and then extracting the main variables required for the SVM classifier that could more clearly identify one condition from other. The advantage of this approach is that it avoids the use of generic mapping functions, which were reported in other publications. The results obtained using the proposed method showed improvements in the overall performance of the LOE protection function.

This paper is organised as follows: in Section 2, the LOE problem is briefly explained. Section 3 explains the SVM concept. Section 4 introduces how this new methodology can be used effectively to identify the LOE condition from power-swing condition and external faults. Section 5 gives the simulation results for different loading conditions, different fault types and with different values for the line impedances. In Section 5, a comparison of results using the proposed method against the traditional two-zone method is also provided. Section 6 gives the final conclusions.

2 LOE protection

An overview describing the main control and protection components of synchronous generator is shown in Fig. 1. Generator protection [21–23] and control must be properly coordinated, so that the control has the ability to perform a corrective action before a protective function decides to shut down the whole generator.

A numerical LOE relay is based on the measurement of voltage and current signals from the generator output terminals. The voltage and current phasors are then calculated and used to estimate the apparent impedance seen by the generator looking into the power system. This impedance is then scaled to a per unit value using the generator ratings as per unit base. An LOE condition is identified when the impedance measured is located in the operating region of this protection function. The operating region of an LOE function typically consists of mho impedance units. A mho impedance unit characteristic for a typical LOE condition is shown in Fig. 2*a*. In Fig. 2*a*, LOE characteristics for heavy and light load conditions are also shown. From Fig. 2*a*, we can see that an LOE condition brings the apparent impedance closer to the negative imaginary axis. The final point of the characteristics shown in the figure corresponds to a point when the generator is about 180° out of phase with the system voltage. This final point is not fixed and its value is between the subsynchronous reactance $-X_d'$ and the synchronous reactance $-X_d$. Therefore the mho impedance zone of the LOE function needs to enclose both points. The resulting mho zone in Fig. 2*a* has the centre located at $(0, \frac{1}{2}(-X'_d - X_d))$ and the radius is $1/2X_d$. In Figs. 2*a* and *b*, it is shown that the time it takes for the impedance to reach the impedance zone depends on the loading of the generator. It takes more time for the impedance to reach the mho zone for lighter load conditions. In Fig. 2*a*, the impedance takes slightly more than 2 s to enter the mho zone for a heavy load condition of $0.80 + j0.41$ pu, whereas this time is about 5 s for a light load condition of $0.05 + j0.01$ pu. However, in Fig. 2*b* the field current I_F has a significant value almost until 3.5 s even though field voltage is zero. In Fig. 2*b*, the heavy load condition becomes loss of synchronism after

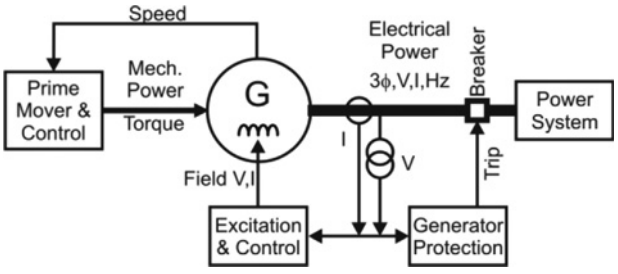

Fig. 1 *Overview showing generator control and protection*

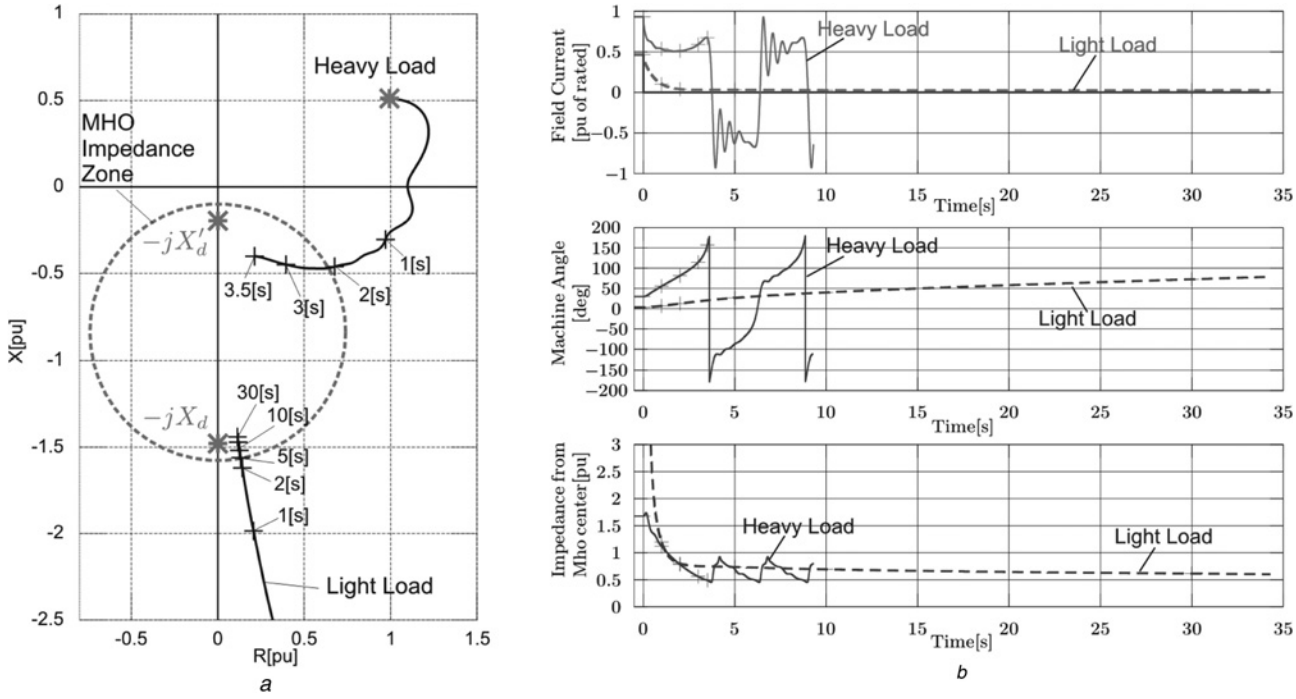

Fig. 2 *Behaviour of LOE condition in the impedance planes and time domain*

a LOE condition
b Field current, machine angle and impedance measured from mho centre for LOE under heavy and light load initial conditions of Fig. 2*a*

3.5 s, producing dangerous transients such as pulsating torque in the shaft of the machine [24]. It must be emphasised that the LOE condition needs to be detected and cleared before loss of synchronism happens, because after that the LOE protection is unable to operate correctly when the impedance increases and leaves the characteristic. In the light load condition, the generator does not lose synchronism until 35 s. This single mho zone LOE typically makes a decision to trip from 1 to 2 s after the impedance enters the mho zone. This mho impedance is not perfectly selective because other conditions may activate it. One such case is the power-swing condition, which may sometimes fall temporarily inside the LOE operating region. Besides, it is desirable to trip faster for the heavy load condition because it is a more severe condition for the generator. Time coordination is used to overcome this problem and is explained below.

A power-swing condition typically enters and leaves the mho impedance zone in a short time compared to the time required for an LOE identification. There are two basic approaches for the detection of an LOE condition:

(a) Two zone [5, 24].
(b) One zone with directional and undervoltage supervision [2, 24].

In the first approach, a second smaller zone of radius 0.5 pu is used to accelerate the trip decision because the probability of a power swing entering the smaller zone is assumed to be very low. However, this need not be the case always as shown in Fig. 3*a* where a stable power-swing condition enters the second smaller zone. In Fig. 3*a*, the initial load at $t = 0$ s is $0.78 - j0.50$ pu, a three-phase fault is applied at 0 s and is cleared at 0.2 s. At ~0.21 s, the impedance enters the two mho impedance zones, leaving the smaller mho zone at 0.53 s and the larger mho zone at 1.15 s. The impedance value settles to the final load beyond 35 s. Fig. 3*b* shows no significant oscillations beyond 4 s. The tripping time for the smaller zone is typically about 0.4 s from the time it enters the smaller zone whereas for the larger zone the tripping time is typically 1–2 s. Therefore it is evident that with these settings, the two zone LOE protection will be able to ride through the power-swing condition without a mal-operation. In the second approach, an undervoltage supervision unit is used instead of a second mho impedance zone. However, the selectivity obtained with the second approach is not as good compared with the two-zone approach [23].

3 Support vector machine

3.1 Theory and method

The SVM is a classification method and has been used for pattern recognition. Fig. 4 illustrates the classification concept using the SVM technique.

The SVM classification is based on linear discriminant functions [25]. A linear discriminant function is one that uses a linear decision boundary surface, that is, a hyperplane, that separates two classes of data. In Fig. 4, hyperplanes H_1 and H_2 separate the two classes of data, whereas hyperplane H_3 does not. The class of the data depends on which side of the hyperplane a given data vector $\boldsymbol{x}_k$ is located. A point $\boldsymbol{x}_p$ located in the hyperplane satisfies (1) where $\boldsymbol{w}$ is the vector normal to the hyperplane. The distance from this plane to the origin is $w_0/\|\boldsymbol{w}\|$

$$\boldsymbol{w}^{\mathrm{T}}\boldsymbol{x}_p + w_0 = 0 \tag{1}$$

The data vector $\boldsymbol{x}_k$ is the pattern to be classified. This vector is also known as a feature vector because its coordinates are the values of key-selected object features to help the classification process. In Fig. 4, the coordinates x_1 and x_2 are the values of

doi: 10.1049/iet-gtd.2012.0340

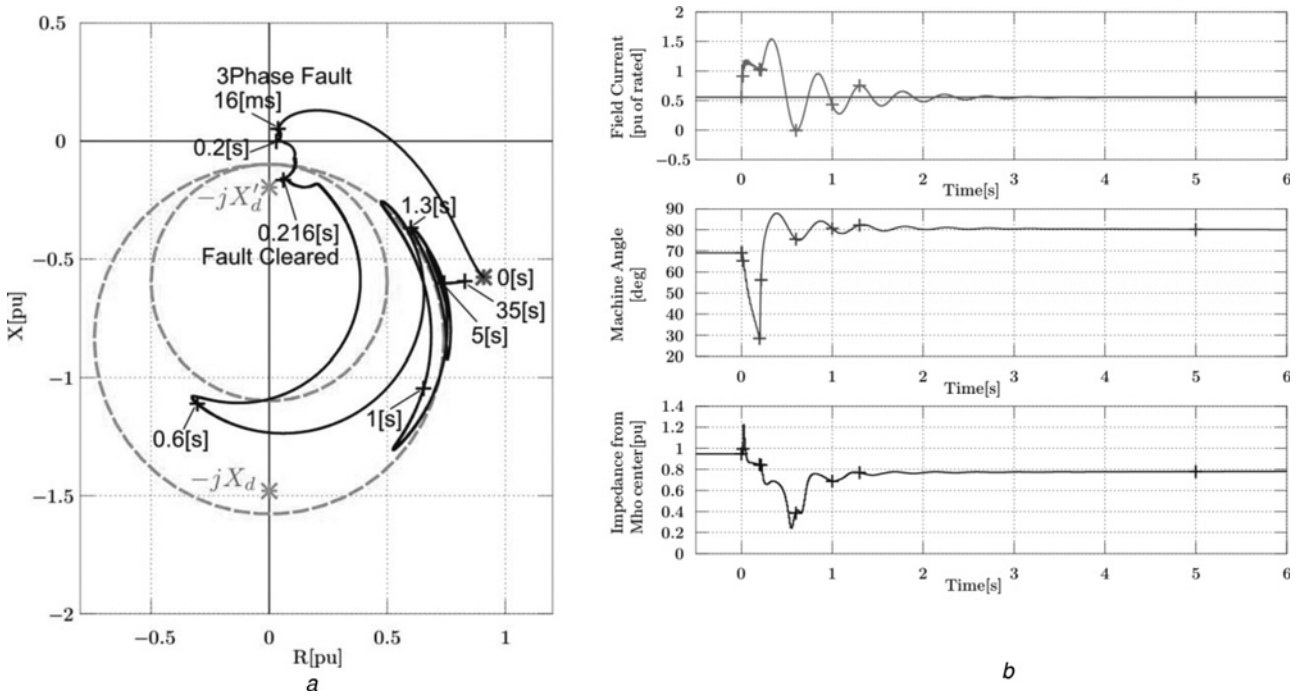

Fig. 3 *Behaviour of power-swing condition in the impedance planes and time domain*

a Stable power-swing condition, leading initial power factor
b Field current, machine angle and impedance measured from mho centre for stable power-swing condition of Fig. 3*a*

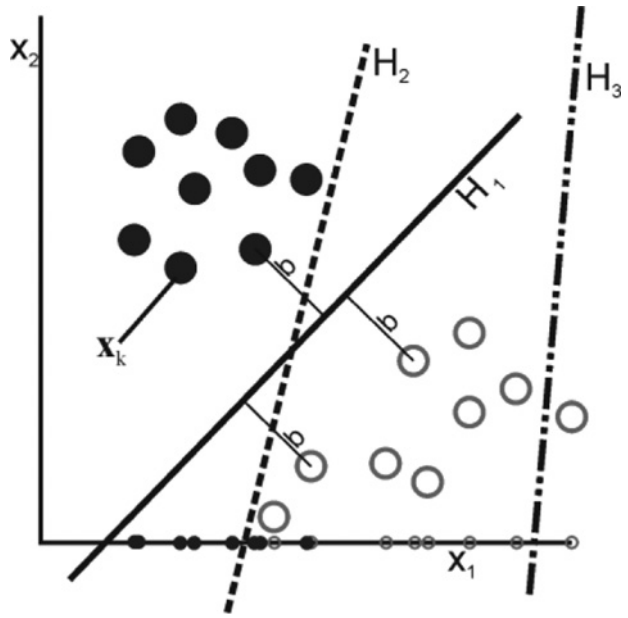

Fig. 4 *Classification concept*

the features used for classification. From Fig. 4, it can be seen that the separation between the two sets of data vectors depends on the quality of the features chosen. For instance in Fig. 4, it is not possible to obtain good classification based on the x_1 coordinate alone; therefore the coordinate x_2 is needed. The distance from a data vector to the hyperplane is given by (2) where b is the minimum distance from any data vector to this hyperplane

$$\left|\frac{\boldsymbol{w}^{\mathrm{T}}}{\|\boldsymbol{w}\|}\left(\boldsymbol{x}_k-\boldsymbol{x}_p\right)\right|=\left|\frac{\boldsymbol{w}^{\mathrm{T}}\boldsymbol{x}_k+w_0}{\|\boldsymbol{w}\|}\right|\geq b \tag{2}$$

The hyperplane parameters $\boldsymbol{w}$ and w_0 are defined, so that the data vector $\boldsymbol{x}_k$ satisfies one of the two inequalities (3) or (4), depending on which side of the hyperplane it is located. The category of a particular data vector $\boldsymbol{x}_k$ is given by the value of z_k. The two inequalities (3) and (4) can be combined into one resulting in (5). Combining (2) and (5) provides the relationship (6) between the minimum distance b and the normal vector $\boldsymbol{w}$

$$\boldsymbol{w}^{\mathrm{T}}\boldsymbol{x}_k+w_0\geq+1\Rightarrow z_k=+1 \tag{3}$$

$$\boldsymbol{w}^{\mathrm{T}}\boldsymbol{x}_k+w_0\leq-1\Rightarrow z_k=-1 \tag{4}$$

$$z_k\left(\boldsymbol{w}^{\mathrm{T}}\boldsymbol{x}_k+w_0\right)\geq+1\quad\forall k \tag{5}$$

$$b=\frac{1}{\|\boldsymbol{w}\|} \tag{6}$$

The training of the classifier consists of finding a hyperplane that separates the two classes of data. The training is performed using vectors from both classes and whose category is known upfront. A trained classifier produces zero classification error when the two classes of data are separable. In a separable case, there may be multiple hyperplanes that separate the two classes. The SVM method finds an optimum separating hyperplane that maximises the distance b. In Fig. 4, both hyperplanes H_1 and H_2 separate the two classes of data, but only H_1 is optimum that maximises the distance b. From (6), this is equivalent to minimising the vector norm $\|\boldsymbol{w}\|$ subject to the constraints (5). Using the Lagrange method to minimise $\|\boldsymbol{w}\|$ results in (7). Note that the Lagrange multipliers α_k in (7) are restricted to values greater or equal to zero because the constraints in (5) are inequalities. Also, note that n is the number of training vectors. From the duality principle, the problem in (7) becomes an optimisation problem

with respect to $\boldsymbol{\alpha}$ instead of with respect to $\boldsymbol{w}$ and w_0 as described in (8). Applying the two conditions in the right-hand side of (8) to the Lagrange function in (7) results in (9) and (10)

$$L(\boldsymbol{w}, w_0, \boldsymbol{\alpha}) = \frac{1}{2}\|\boldsymbol{w}\|^2 - \sum_{k=1}^{n} \alpha_k \left[z_k\left(\boldsymbol{w}^{\mathrm{T}}\boldsymbol{x}_k + w_0\right) - 1\right]; \quad \alpha_k \geq 0 \quad \forall k \tag{7}$$

$$\min_{\boldsymbol{w}, w_0, \nabla_\alpha L = 0} L(\boldsymbol{w}, w_0, \boldsymbol{\alpha}) \leftrightarrow \max_{\boldsymbol{\alpha}, \nabla_w L = 0, \partial L/\partial w_0 = 0} L(\boldsymbol{w}, w_0, \boldsymbol{\alpha}) \tag{8}$$

$$\nabla_{\boldsymbol{w}} L = 0 \rightarrow \boldsymbol{w} = \sum_{k=1}^{n} \alpha_k z_k \boldsymbol{x}_k \tag{9}$$

$$\frac{\partial L}{\partial w_0} = 0 \rightarrow \sum_{k=1}^{n} \alpha_k z_k = 0 \tag{10}$$

Substituting (9) and (10) into (7) gives (11); which is subject to the constraints given by (12)

$$L(\boldsymbol{\alpha}) = \sum_{k=1}^{n} \alpha_k - \frac{1}{2}\sum_{k=1}^{n}\sum_{l=1}^{n} \alpha_k \alpha_l z_k z_l \boldsymbol{x}_k \boldsymbol{x}_l \tag{11}$$

$$\sum_{k=1}^{n} \alpha_k z_k = 0; \quad \alpha_k \geq 0 \quad \forall k \tag{12}$$

Solution of (11) and (12) requires solving a quadratic programming problem of the form given in (13). This kind of problem can be solved using any numerical optimisation method. In this paper, a null-space active-set method is used

$$L(\boldsymbol{\alpha}) = -\frac{1}{2}\boldsymbol{\alpha}^{\mathrm{T}}\boldsymbol{H}\boldsymbol{\alpha} + \boldsymbol{c}^{\mathrm{T}}\boldsymbol{\alpha} \tag{13}$$

where

$$H_{kl} = z_k z_l \boldsymbol{x}_k \boldsymbol{x}_l; \quad k,\ l = 1, .., n$$
$$\boldsymbol{c}^{\mathrm{T}} = \begin{bmatrix} 1 & 1 & \cdots & 1 \end{bmatrix}_{1xn}$$

Once $\boldsymbol{\alpha}$ is known the values of $\boldsymbol{w}$ and w_0 are easily obtained using (9) and (5). The data vectors $\boldsymbol{x}_k$ located exactly at a distance b from the hyperplane are known as support vectors. The Lagrange multipliers α_k corresponding to the support vectors may be greater than zero whereas all other multipliers must be zero. The number of support vectors is typically much less than the total number of training vectors.

If the data are not separable in the original space, mapping functions are used such as polynomial functions, Gaussian functions etc. By doing this, the vectors can be mapped to a higher dimension space where the two classes are linearly separable. In this new mapped space, the hyperplane is constructed and the methods described before can be applied to find the SVM classifier. Compared to the ANN, the SVM has the advantage that it is not as complex and the training needs are not as demanding. In this work, superior classifications could be achieved with an SVM by proper selection of input features without the need for applying a more complex ANN.

4 Application of SVM to LOE protection

An alternative approach to the traditional time coordination is proposed in this work. From Figs. 2 and 3, we can see that the trajectories for an LOE condition and for a power-swing condition have some noticeable differences. These differences are with respect to the path and the duration for the two types of disturbances in the complex plane plot (Figs. 2 and 3). One of the contributions of this paper is the identification of these differences for finding the appropriate features and is described in detail in the following Section 4.1.

As discussed in the introduction, this paper uses the SVM pattern recognition method for identifying an LOE from a stable power swing or other conditions. With this new approach, there is no need to use additional elements such as:(i) second smaller zone, and (ii) directional or undervoltage elements. Also, time coordination is improved.

4.1 Feature selection

The features are based on measurements of the fundamental frequency voltage and current made over a given time window. These measurements are taken at several points and are evenly distributed in this time window. In this work, 20 points (V_k, I_k, $k = 0,\ldots,19$) distributed evenly over a 1 s time window were selected. It should be noted that 1 s is a typical time used in the coordination of an LOE function with power-swing conditions.

Two kinds of plots in the complex plane are typically used in the study of LOE conditions, the power plane and the impedance plane. The power and impedance values are commonly scaled to per unit using the generator ratings as the base for the calculation. The discrete Fourier transform (DFT) method with a sampling rate of 256 samples per cycle is used to obtain phasors V and I.

As discussed before, one of the key contributions of this paper is in finding the actual features that are useful in identifying a power swing from an LOE condition. This was based on observing the trajectories of the two conditions in the complex power plane and the impedance plane.

The first feature was obtained by looking at the trajectories in the impedance plane. In Figs. 2 and 3, the points outside of the mho zone are not considered an LOE condition. Therefore one feature chosen is the distance in the impedance plane from the most recent point in the 1 s window to the centre of the traditional large mho zone, as described in (14). In (14), Z_{19} is the most recent impedance measurement in the 1 s window. However, this feature alone is not enough for a complete classification, because in cases such as that of Fig. 3, a power-swing condition may enter the mho zone

$$x_1 = \left| Z_{19} - \frac{\left(-\mathrm{j}X_d - \mathrm{j}X_d'\right)}{2} \right| \tag{14}$$

The next two features are found by looking at the behaviour of LOE condition and the power-swing condition in the power plane as shown in Figs. 5 and 6. In Figs. 5 and 6, the generator capability curve (GCC) is plotted as a reference at rated voltage conditions. The GCC is not constant and varies with generator terminal voltage. From Fig. 6*a*, we can see that the trajectory for an LOE follows a negative imaginary direction. However, this behaviour is only valid up to the time the machine loses synchronism at

doi: 10.1049/iet-gtd.2012.0340

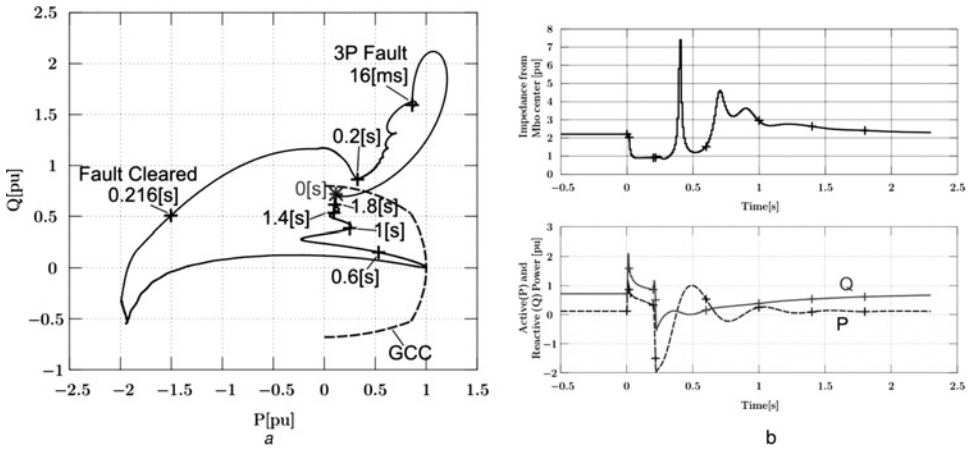

Fig. 5 *Behaviour of power-swing condition in the power planes and time domain*

a Stable power-swing condition, lagging initial power factor
b Impedance, active and reactive power for the stable power-swing condition of Fig. 5*a*

about 3.5 s as seen in Fig. 6*b*. On the contrary, in Fig. 5, the trajectory for a power swing ($t > 0.216$ s) follows a positive imaginary direction if we disregard the prefault condition ($t < 0$ s), transition between prefault to fault condition ($t = 0$. s–16 ms), fault condition ($t = 16$ ms–0.2 s) and the transition from fault into the power swing ($t = 0.2$–0.216 s). Therefore the next feature is chosen as the imaginary component of the total displacement in the 1 s window, as described in (15). In (15), S_0 and S_{19} are the earliest and the most recent apparent power measurement points, respectively, in the 1 s window. It should be noted again that this feature alone is not enough to classify an LOE condition correctly because the 1 s window includes the transition and the fault conditions that have to be isolated

$$x_2 = \Im\{S_{19} - S_0\} \tag{15}$$

From Figs. 5 and 6, we also note that an LOE has a more direct path, that is, closer to a straight line, compared with a power-swing condition. By a more direct path, it means that the value of the total length travelled in the path for a given time window is closer to the value of the length of a direct straight line from start to end of that path. Therefore the feature is chosen as the ratio between these two values and is described mathematically in (16). The value of the ratio for a more direct path is going to be a number closer to 1.0.

$$x_3 = \frac{\sum_{i=1}^{19} |S_i - S_{i-1}|}{|S_{19} - S_0|} \tag{16}$$

The feature just described above is useful in identifying the power-swing condition period (Fig. 5). Let us consider the time window 0.216–1.216 s in Fig. 5. This time window includes the power-swing condition. It can be easily seen that the value of x_3 is going to be much larger than 1.0.

It is interesting to mention that the characteristic during the transition periods from prefault to fault (0.2–0.225 s) and from fault into the power swing (0.4–0.425 s) are mostly

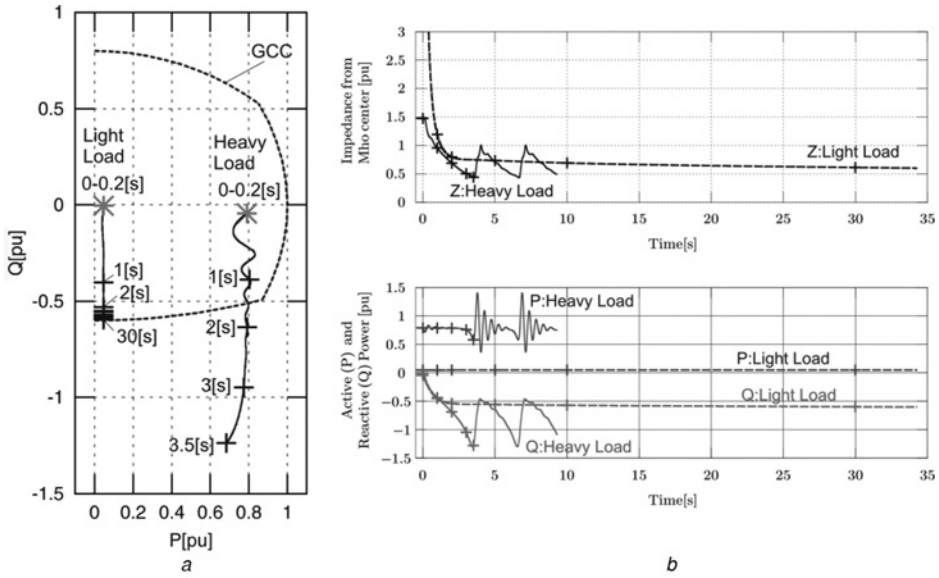

Fig. 6 *Behaviour of LOE condition in the power planes and time domain*

a LOE condition, power factor close to unity
b Impedance, active and reactive power for the LOE conditions of Fig. 6*a*

influenced by the response of the full cycle DFT phasor estimation method. For instance, the transition from prefault to fault is practically instantaneous in the time domain, that is, a fraction of a millisecond. During this transition, the DFT window uses samples collected from prefault and fault, therefore producing phasor values in between these two conditions.

It was found that the first three features were able to classify the LOE condition from other conditions in most of the cases, except during the transition periods just described. To overcome this, an additional feature was chosen and this feature is described below.

From Figs. 6*a* and 6*b*, we see that the point in the path moves relatively slow during an LOE condition, before loss of synchronism occurs. That is, no large sudden changes are observed during an LOE condition. This fact is included as a feature and is chosen based on the maximum change in the path over two consecutive points during the 1 s window. Then the fourth feature is calculated as the distance that would be travelled if that maximum change was constant over the 1 s as described in (17). A faster movement produces a larger value of this feature.

$$x_4 = (N-1)\max\left(\left|S_i - S_{i-1}\right|\right), \quad N = 20,\ i \in [1..(N-1)] \tag{17}$$

Overall, the feature vector proposed has four coordinates, as shown in (18) and each coordinate is described mathematically by the relationships (14)–(17)

$$\boldsymbol{x}_k = \begin{bmatrix} x_1 & x_2 & x_3 & x_4 \end{bmatrix} \tag{18}$$

The performance of the features presented for LOE of Fig. 6 and for stable power-swing conditions of Fig. 5 are illustrated in Figs. 7*a* and *b*. The first feature drops below 1.0 pu during an LOE condition before a loss of synchronism happens. However, this same feature also drops temporarily during a power-swing condition. The second feature is negative during an LOE condition, although its value eventually becomes very small for a light load condition. During a power-swing condition this feature also may become negative temporarily. The third feature is a value close to 1.0 for an LOE condition. This feature is larger than 1.0 during a power swing, but this difference is not so noticeable while the fault is present ($t = 0$–0.2 s). The fourth feature is clearly about 1.0 pu during the LOE condition. This same feature is larger than 10 pu for a stable power-swing condition, helping specially during periods of rapid change in the variables considered.

The traditional application of SVMs use generic higher dimension mapping functions such as the Gaussian or polynomial [25] function to separate the data vectors. However, the features described in (18) were obtained by looking at the actual characteristics and were nothing but mapping of original time-domain samples instead of just using generic mapping functions as it is. This helped in obtaining better classification accuracy and the results are given later in Section 5.

4.2 Training considerations

The training consists of finding the hyperplane parameters $\boldsymbol{w}$ and w_0 of the desired classifier using the SVM method.

4.2.1 Power system modelling: A generator connected to an infinite bus through a power line is used. A time-domain model of the synchronous machine using dq_0 transformation is used to represent the generator. The mechanical behaviour is represented by a lumped mass. The prime mover and excitation controls are set in a manual mode during the simulation and the reason is as follows. For prime mover control, the time constants are relatively large compared to the simulation time so there is no need to include the prime mover dynamics in the simulation model. When the excitation control is in manual mode, the worst swing scenarios can be generated easily. Here worst swing condition means that the impedance obtains closer and inside of the LOE impedance region during a stable power-swing condition [5]. The power line is represented by a lumped impedance. A fault resistance is connected at 50% of the line. For simplicity, a step up transformer is not included. Beside, the proposed method is expected to work with or without the presence of this power transformer.

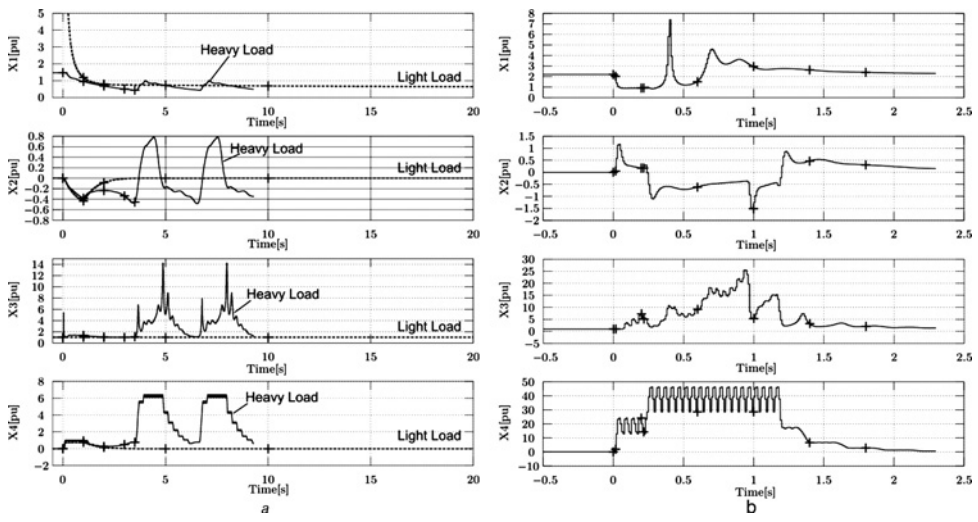

Fig. 7 *Features presented for LOE and stable power-swing conditions*

a Features behaviour for the LOE conditions of Fig. 6
b Features behaviour for the stable power-swing condition of Fig. 5

doi: 10.1049/iet-gtd.2012.0340

4.2.2 Initial conditions: To make the classifier more general, the training cases consider all limits of the GCC. A total of six cases are used, combining load and power factor variations such as high and light load and leading, lagging and unity power factor. To achieve these initial load conditions, two parameters are varied:

1. Voltage magnitude, within ±5%.
2. Angle, within 90° stability limit and the generator is leading the infinite bus.

4.2.3 Selection of disturbances: Stable power-swing conditions are obtained by applying a three-phase short circuit, and removing it after a short period of time. Although producing the power swing cases, the following two considerations are taken into account:

1. The impedance enters temporarily the LOE mho zone during the power swing.
2. The system actually recovers, that is, returns to a stable condition.

The LOE conditions are obtained by using the following sequence:

1. Starting with an initial load, the field voltage is adjusted to produce the desired load conditions in the *PQ*-plane.
2. Zero the field voltage until the end of the simulation period.

4.2.4 Simulation: The alternative electromagnetic transient programme (ATP/EMTP) is used to obtain the time domain solution of the model described above [26]. A solution time step of 65.1 μs, equivalent to 256 samples every power-system cycle, is used for this. This time-step allows us to properly reproduce a bandwidth of 0.00–7.68 kHz. Thus, most of the transients are considered. The total time duration of simulation is chosen such that both kinds of disturbances can be observed clearly: the LOE and the power swing. In case of a power swing, it is important to verify that the generator returns back to a stable condition. It should be noted that unstable power swings of any kind are not considered in this work as this condition is typically detected by other protection functions, such as out-of-step relays [5]. It should be also noted that during a power swing, the fundamental frequency at the generator terminal may vary significantly (±1.0 Hz or more). In case of an LOE condition, it is also important to confirm if and when a loss of synchronism follows.

4.2.5 Selection of data vectors: After the simulation is done, the data vectors are calculated and consolidated as described in Section 4.1, using the mathematical programme Octave. As described before, the impedance characteristics present a more direct path when they start approaching the mho zone and, therefore the following three restrictions are taken into consideration for choosing the training vectors:

1. During a heavy loading condition, the training vector is chosen from the instant when the most recent of the 20 points on the characteristic is just inside the mho zone (Fig. 2).
2. For lightly loaded cases, the first 1 s from the beginning of an LOE disturbance is disregarded (Fig. 2).
3. The loss of synchronism that may follow an LOE condition is not included as discussed before.

For a stable-power-swing condition, all possible data vectors are used without restrictions. This means that the prefault, fault, power swing and final load data vectors are included. Also, the transitions between these conditions are included. The resulting classifier is actually trained to identify a non-LOE condition instead of just a stable-power-swing condition.

4.2.6 SVM solution: In this work, the numerical solution is obtained using the quadratic programming function *qp*() from the mathematical programme Octave. First $\boldsymbol{\alpha}$ is obtained and then $\boldsymbol{w}$ and w_0 are obtained, as described in Section 3.1. Once $\boldsymbol{w}$ and w_0 are obtained, the classifier is verified using (20) for all training data vectors. A zero classification error confirms that the data are separable in the original space.

5 Studies and results

To demonstrate improvements are achievable, the proposed method is applied to a 104.4 MVA, 13.8 kV, 3600 rpm and wye connected synchronous generator as described in Section 4.2.1. The synchronous machine parameters of this generator are given in Appendix. This generator is connected to the infinite bus through a line of $0.11\angle 84.3°$ pu impedance in generator base units. A fault resistance of 0.005 pu is used, which is connected at 50% of the line.

5.1 Training data and resulting SVM classifier

The data vectors used for training are taken from both classes of disturbances: stable power swing and LOE. To produce the stable power swing, the three-phase fault is applied at $t = 0$ s and removed at 200 ms in the simulation time scale. To produce the LOE, the field voltage is reduced to zero at $t = 0$ s in the same time scale. The total length of simulation used is of 35 s. The duration of power swing observed is between 2 and 5 s. The duration of LOE depends on the loading condition. For high load, the LOE lasts between 2.8 and 3.7 s before a loss of synchronism happens. For a light load, the LOE may not cause loss of synchronism within the 35 s observed.

A total of 116 data vectors are used for the training. These cases are listed in Table 1. After the training vectors are specified, the SVM equation is solved. A total of four support vectors are obtained with two stable power swings and two LOE. The parameters of the resulting classifier are given in (19) and (20). The classification error is then verified using the training vectors and the two classes are confirmed to be separable

$$\boldsymbol{w}^{\mathrm{T}} = \begin{bmatrix} 17.6668 & 238.786 & 6.1026 & 22.7685 \end{bmatrix} \quad (19)$$

$$w_0 = -19.730 \quad (20)$$

5.2 SVM implementation

In this work, the method described in Section 4.1 is implemented using Foreign Models compiled object in ATP. Two methods of LOE detection were implemented in this foreign models object for performance comparison: (a) the SVM classifier, and (b) the traditional two mho zone LOE. The phasor estimation was

Table 1 Simulation runs and training data vectors

Case no.	Load/PF	Initial P +jQ, pu	Number of vectors	Type of case	
1	light/lagging	0.12 + j0.72	8	LOE	47
2	light/unity	0.05 – j0.01	10	LOE	vectors
3	light/leading	0.03 – j0.55	11	LOE	
4	heavy/lagging	0.80 + j0.41	6	LOE	
5	heavy/unity	0.79 – j0.04	3	LOE	
6	heavy/leading	0.78 – j0.50	9	LOE	
7	light/lagging	0.12 + j0.72	8	PS-3P	69
8	light/unity	0.05 – j0.01	8	PS-3P	vectors
9	light/leading	0.03 – j0.55	10	PS-3P	
10	heavy/lagging	0.80 + j0.41	12	PS-3P	
11	heavy/unity	0.79 – j0.04	14	PS-3P	
12	heavy/leading	0.78 – j0.50	17	PS-3P	

PS: power swing, 3P: three-phase fault used.

implemented using DFT with angle normalisation, so that a steady-state fundamental frequency condition produces a fixed phasor value. The three phases of current and voltage were used to obtain the positive-sequence current and voltage phasor. These positive-sequence phasors are used by the SVM method described. The SVM classifier is defined mathematically by (3) and (4) using the parameters (19) and (20) obtained from the SVM solution. The output of this classifier in time is used to assess the performance.

5.3 Test considerations and results

5.3.1 New cases similar to the training cases: These cases are obtained using the same disturbances that were used for training. In Table 2, the SVM method is compared with the traditional LOE detection. The SVM pickup time is the time it takes for the proposed method to confirm that it is an LOE condition. The SVM reset time also indicates the time when loss of synchronism happens. In these cases, good results are more likely because of the similarity of the data vectors with the ones used for training.

5.3.2 New cases (different initial conditions and different types of faults): These new cases are obtained by modifying the conditions or parameters of the system to which the generator is connected, such as initial load conditions, fault types that produce power swing and modifying the line length connecting the infinite bus.

5.3.2.1 Different initial loads: Two different initial load conditions are used for the new cases. For each of these conditions, one LOE scenario and one power-swing scenario is generated, and are listed in Table 3.

5.3.2.2 Different fault types: The power swing scenarios generated so far used three-phase fault types. However, unbalanced faults occur more frequently in reality. Thus, it is important to verify the performance of SVM during unbalanced fault conditions as well. Four more cases with the following fault types are used: AG, BG, ABG and BCG. The four cases are listed in Table 4. To bring the impedance during power swing closer or inside of the LOE characteristic, the worst case scenario of the six initial load conditions is used, that is, a heavy load with leading power factor (0.78 – j0.50 pu). The worst case scenario used in this work was described by Berdy [5] as voltage regulator out of service, low-system impedance, fault clearing time equal to critical switching time (i.e. the maximum switching time for which the machine is stable) and the machine operating at the leading power factor.

5.3.2.3 Different power line: The electrical centre of the power swing moves away from the generator when the line length is increased while the electrical centre moves closer to the generator impedance or may fall inside the generator impedance when the line length is reduced. When the electrical centre is too far from the generator impedance, then the power swing may not enter the LOE region. The length of the power line that connects to the infinite bus was, therefore increased from 0.11 to 0.33 pu. Beyond 0.33 pu line length, the power swing did not enter the LOE impedance zone. Only four initial load conditions are used combining load and power factor variations: heavy/light load and leading/lagging power factor. Eight more cases are produced: four power swing and four LOE, they are listed in Table 5. The power swing is produced using only three-phase faults in this part.

5.3.3 Sensitivity of proposed method to generator parameters accuracy: The parameters of the generator

Table 2 New cases similar to training cases

				Two MHO zone						
				Large MHO time, s		Small MHO time, s		SVM (time, s)		
Case no.	Load/PF	Initial P+jQ, pu	Type of case	Pickup	Trip	Pickup	Trip	Pickup	Reset	Loss of synch. time, s
1	LL/lag.	0.12 + j0.72	LOE	7.7222	8.7133	–	–	0.26739	24.410	25
2	LL/unity	0.05 – j0.01	LOE	4.5423	5.5335	–	–	0.40160	–	–
3	LL/lead.	0.03 – j0.55	LOE	0.9520	1.9432	–	–	0.22071	–	–
4	HL/lag.	0.80 + j0.41	LOE	2.1591	3.1502	2.7405	3.1304	0.21257	3.7512	3.76
5	HL/unity	0.79 – j0.04	LOE	1.7824	2.7735	2.5027	2.8924	0.24161	3.6203	3.62
6	HL/lead.	0.78 – j0.50	LOE	0.7758	1.7603	1.6612	2.0511	0.4207	2.8707	2.87
				Pickup	Reset	Pickup	Reset	Pickup	Reset	
7	LL/lag.	0.12 + j0.72	PS-3P	–	–	–	–	–	–	–
8	LL/unity	0.05 – j0.01	PS-3P	0.2709	0.31055	–	–	–	–	–
8(*)				0.5121	0.63103					
9	LL/lead.	0.03 – j0.55	PS-3P	0.25554	2.8282	0.26433	0.77536	–	–	–
10	HL/lag.	0.80 + j0.41	PS-3P	0.26433	0.29076	–	–	–	–	–
11	HL/unity	0.79 – j0.04	PS-3P	0.25554	0.33483	0.25554	0.31719	–	–	–
12	HL/lead.	0.78 – j0.50	PS-3P	0.24668	0.76651	0.24668	0.56385	–	–	–
12(*)				0.88108	1.1630					

LL: light load, HL: heavy load, PS: power swing, 3P: three-phase fault used, (*) picked up twice.

doi: 10.1049/iet-gtd.2012.0340

Table 3 Different initial load conditions

Case no.	Load/PF	Initial P+jQ, pu	Type of case	Two MHO zone						Loss of synch. time, s
				Large MHO time, s		Small MHO time, s		SVM time, s		
				Pickup	Trip	Pickup	Trip	Pickup	Reset	
13	ML/lag.	0.37 + j0.47	LOE	3.8274	4.8165	6.0143	6.4099	0.6429	7.5702	7.56
14	ML/lead.	0.38– j0.30	LOE	3.1615	4.1462	6.5308	6.9154	0.3425	8.1902	8.13
				Pickup	Reset	Pickup	Reset	Pickup	Reset	
15	ML/lag.	0.37 + j0.47	PS-3P	0.26433	0.32598	0.27311	0.29076	–	–	–
16	ML/lead.	0.38– j0.30	PS-3P	0.24668	0.56385	0.25554	0.47577	–	–	–

ML: medium load, PS: power swing, 3P: three-phase fault used.

Table 4 Unbalanced fault types

Case no.	Load/PF	Initial P+jQ, pu	Type of case	Two MHO zone						Loss of synch. time, s
				Large MHO time, s		Small MHO time, s		SVM time, s		
				Pickup	Reset	Pickup	Reset	Pickup	Reset	
17	HL/lag.	0.78 – j0.50	PS-AG	0.24668	0.39648	0.24668	0.31719	–	–	–
18	HL/lead.	0.78 – j0.50	PS-BG	0.2379	0.39648	0.24668	0.3084	–	–	–
19	HL/lag.	0.78 – j0.50	PS-ABG	0.2379	0.60792	0.2379	0.36126	–	–	–
20	HL/lead.	0.78 – j0.50	PS-BCG	0.2379	0.62557	0.24668	0.37005	–	–	–

HL: heavy load, PS: power swing, AG/BG/ABG/BCG fault type used.

could be determined to a certain degree of accuracy, depending on the method used to obtain those values. Therefore it is important to study the stability of the proposed method to small variations in the generator parameters. The cases for most severe LOE event (case no. 6 in Table 2) and corresponding power swing (case no. 12 in Table 2) were used to study the sensitivity of the proposed method. A variation of either ±5% was used, depending on which one caused the operating point to enter the LOE mho zone, that is, more risk of mal-operation. The results are given in Table 6.

The parameter that affected the detection of an LOE condition the most (case no. 6 of Table 2) by the SVM method proposed was an increase in the X_q' of 5%. The impact was a delay of 33 ms in the detection as indicated in Table 6. For the same LOE condition, the traditional two-zone mho impedance method was also affected by the parameter variation, but resulted in a faster trip time by 33 ms for an increase in the rated voltage 5%. However, the overall decision time using the SVM method was still faster (453 ms) compared to the traditional two-mho zone method (1.73 s).

On the other hand, for a power-swing condition (case no. 12 of Table 2) the SVM was not affected. The SVM classifier successfully and clearly identified all the instances where the impedance entered the LOE mho zone as a non-LOE condition. However, the traditional two-mho zone method was affected, because the machine was operating very close to the transient stability limit. This limit depends on two variables: the point in the PQ-plane relative to the GCC curve and the fault duration. The point in the PQ-plane in this case is on the limit of the GCC curve in the leading reactive region and the fault duration used for

Table 5 Longer line

Case no.	LOAD/PF	Initial P+jQ, pu	Type of case	Two MHO zone						Loss of synch. time, s
				Large MHO time, s		Small MHO time, s		SVM time, s		
				Pickup	Trip	Pickup	Trip	Pickup	Reset	
21	HL/lead.	0.60 – j0.28	LOE	1.6436	2.6348	2.4102	2.8066	0.5417	3.3355	3.34
22	HL/lag.	0.66 + j0.32	LOE	2.582	3.5731	2.952	3.3441	0.28015	3.6062	3.62
23	LL/lead.	0.02 – j0.29	LOE	2.6826	3.6739	–	–	0.4739	–	–
24	LL/lag.	0.08 + j0.31	LOE	8.6903	9.682	–	–	4.9332	28.186	28.0
				Pickup	Reset	Pickup	Reset	Pickup	Reset	
25	HL/lead.	0.60 – j0.28	PS-3P	0.55506	0.85465	–	–	–	–	–
26	HL/lag.	0.66 + j0.32	PS-3P	–	–	–	–	–	–	–
27	LL/lead.	0.02 – j0.29	PS-3P	0.26433	0.68722	–	–	–	–	–
28	LL/lag.	0.08 + j0.31	PS-3P	–	–	–	–	–	–	–

LL: light load, HL: heavy load, PS: power swing, 3P: three-phase fault type used.

Table 6 Sensitivity to generator parameters

Case no.	Parameter varied	Initial P+jQ, pu	Type of case	Two MHO zone						Loss of synch. time, s
				Large MHO time, s		Small MHO time, s		SVM time, s		
				Pickup	Trip	Pickup	Trip	Pickup	Reset	
6	–	0.78 – j0.50	LOE	0.7758	1.7603	1.6612	2.0511	0.4207	2.8707	2.87
	MVA + 5%			0	+11 ms	+77 ms	+88 ms	−11 ms	+22 ms	
	kV + 5%			−33 ms	−33 ms	−198 ms	−176 ms	0	−407 ms	
	X_d + 5%			−22 ms	−22 ms	−77 ms	−55 ms	−11 ms	−110 ms	
	X_q + 5%			+11 ms	+11 ms	−11 ms	0	+33 ms	−55 ms	
	X_d' + 5%			0	0	−22 ms	−11 ms	−11 ms	−22 ms	
	X_q' + 5%			0	0	−22 ms	−11 ms	−11 ms	−33 ms	
	X_d' + 5%			0	0	−11 ms	0	−11 ms	−11 ms	
	X_q' + 5%			0	0	−11 ms	0	−11 ms	−11 ms	
	T_{do}' + 5%			+33 ms	+33 ms	+55 ms	+66 ms	−11 ms	+110 ms	
	T_{qo}' + 5%			0	0	−11 ms	+11 ms	−11 ms	+11 ms	
	T_{do}' + 5%			0	11 ms	−11 ms	0	−11 ms	0	
	T_{qo}' + 5%			0	0	−11 ms	+11 ms	−11 ms	+11 ms	
	H + 5%			0	0	−11 ms	0	−11 ms	0	
				Pickup	Reset	Pickup	Reset	Pickup	Reset	
12	–	0.78 – j0.50	PS-3P	0.1913	0.6304	0.1913	0.3826	–	–	
	MVA – 5%			0	0	0	+28.2 ms	–	–	
	kV + 5%			−11 ms	+12 ms	−11 ms	+59 ms	–	–	
	X_d + 5%			0	+2 ms	0	+10 ms	–	–	
	X_q + 5%			0	+1 ms	0	+19 ms	–	–	
	X_d' + 5%			0	0	0	−2 ms	–	–	
	X_q' + 5%			0	0	0	−22 ms	–	–	
	X_d' + 5%			+1 ms	0	+1 ms	0	–	–	
	X_q' + 5%			0	+2 ms	0	−1 ms	–	–	
	T_{do}' + 5%			0	0	0	−11 ms	–	–	
	T_{qo}' + 5%			0	+1 ms	0	−2 ms	–	–	
	T_{do}' + 5%			0	0	0	−2 ms	–	–	
	T_{qo}' + 5%			+1 ms	0	+1 ms	−1 ms	–	–	
	H + 5%			0	0	0	−11 ms	–	–	

LL: light load, HL: heavy load, PS: power swing, 3P: three-phase fault type used.

all prior cases is 200 ms. The parameters that caused the most impact on the performance of the traditional LOE detection method for this power-swing condition were 5% variation of in the MVA rating, the kV rating and the X_d synchronous reactance, which made the machine to lose synchronism for the fault duration of 200 ms being used. It is unlikely a machine is going to be operated so close to the transient stability limit, thus the fault duration time was reduced from 200 to 150 ms, so that there was no loss of synchronism.

5.4 Comparison of SVM technique with traditional technique

From the cases tested, the SVM method is able to identify the LOE condition before the impedance enters the mho zone. However, for increased security, a trip decision can be made when the impedance just enters the LOE mho zone. The traditional method uses time coordination, which starts only when the impedance enters either of the two-mho zones, thus it takes longer than using the proposed SVM method. Taking for instance the case no. 4, shown in Fig. 2*a*, the impedance takes 2.16 s to reach the mho impedance zone. The proposed SVM method detects this condition at just 213 ms. The traditional two zone LOE needs to wait 1 s after the impedance enters the zone and then trips only at 3.13 s. It should be noted that although the SVM method proposed uses a 1 s window, it can detect an LOE with less than 1 s of disturbance information. Also, it should be noted that the improvements are more significant for the heavier load conditions and less significant for the lighter load conditions.

6 Conclusions

The traditional LOE protection function relies on time coordination and extra protection elements to ensure that no other disturbances cause an incorrect operating decision. A new method to identify the LOE from power swing disturbances was presented in this paper. This method was based on the SVM pattern recognition technique. A careful selection of identifying features was done to take full advantage of the capabilities of the SVM method. The resulting classifier provided accurate identification for various operating conditions of the synchronous generator. By combining this classifier with the traditional one-zone mho impedance, it was shown that detection time for identifying the LOE condition was significantly improved compared to the traditional two-mho zone method without any loss of accuracy of detecting the LOE condition.

7 Acknowledgments

A part of this work was presented in the student poster competition during the IEEE PES General Meeting in Calgary, Canada, July 2009 [27].

8 References

1 Mason, C.R.: 'A new loss-of-excitation relay for synchronous generators', *AIEE Trans. III, Power Appar. Syst.*, 1949, **68**, pp. 1240–1245
2 Tremaine, R.L., Blackburn, J.L.: 'Loss-of-field protection for synchronous machines', *AIEE Trans. III, Power Appar. Syst.*, 1954, **73**, (1), pp. 765–772

doi: 10.1049/iet-gtd.2012.0340

3 Bisbee, J.M., Rosol, M.F., Wagner, C.L., *et al.*: 'A partial survey of relay protection of steam-driven A-C generators', *AIEE Trans III, Power Appar. Syst*, 1962, **80**, pp. 954–957
4 Mackenzie, W.F., Imhof, J.A., Dewey, C., *et al.*: 'Loss-of-field relay operation during system disturbances working group report – June 1971', *IEEE Trans. Power Appar. Syst.*, 1975, **PAS-94**, (5), pp. 1464–1472
5 Berdy, J.: 'Loss of excitation protection for modern synchronous generators', *IEEE Trans. Power Appar. Syst.*, 1975, **PAS-94**, (5), pp. 1457–1463
6 Lee, D.C., Kundur, P., Brown, R.D.: 'A high speed, discriminating generator loss of excitation protection', *IEEE Trans. Power Appar. Syst.*, 1979, **PAS-98**, (6), pp. 1895–1899
7 Herrman, H.J., Smit, A.: 'Increased sensitivity of loss of field protection based on admittance measurement'. Western Protective Relay Conf., Washington State University, 2009, pp. 1–15
8 Tambay, S.R., Paithankar, Y.G.: 'A new adaptive loss of excitation relay augmented by rate of change of reactance'. Proc. IEEE Power Engineering Society General Meeting (PES-GM), June 2005, vol. 2, pp. 1831–1835
9 Li, L., Caixin, S., Daohuai, M.: 'Study on the excitation protection and control of synchronous generator based on the delta and s'. Proc. IEEE PES Transmission and Distribution Conf. Exhibition: Asia and Pacific, August 2005, pp. 1–4
10 Usta, O., Musa, M.H., Bayrak, M., *et al.*: 'A new relaying algorithm to detect loss of excitation of synchronous generators', *Turk. J. Eletr. Eng.*, 2007, **15**, (3), pp. 339–349
11 Yaghobi, H., Mortazavi, H., Ansari, K., *et al.*: 'A novel flux-based method for synchronous generator loss of excitation protection'. Proc. 25th Int. Power System Conf. (PSC 2010), 2010, pp. 1–14
12 Shi, Z.P., Wang, J.P., Gagic, Z., *et al.*: 'The comparison and analysis for loss of excitation protection schemes in generator protection'. Int. Conf. on Developments in Power System Protection (DPSP), 2012, pp. 1–6
13 Lee, C.H., Ma, L.S., Weng, C.H., *et al.*: 'Lessons learned from the generator loss of field at a cogeneration thermal plant in Taiwan', *IEEE Transactions on Power Systems*, 2011, **26**, (4), pp. 2093–2100
14 Siwang, Y., Weijian, W., Ling, L., *et al.*: 'Discussion on setting calculation of loss-of-excitation protection for large turbogenerator'. Int. Conf. on Electrical Machines and Systems (ICEMS), 2010, pp. 1413–1416
15 Sharaf, A.M., Lie, T.T.: 'ANN based pattern classification of synchronous generator stability and loss of excitation', *IEEE Trans. Energy Convers.*, 1994, **9**, (4), pp. 753–759
16 So, K.H., Heo, J.Y., Aggarwal, R.K., Song, K.B.: 'Out-of-step detection algorithm using frequency deviation of voltage', *IET Gener. Transm. Distrib.*, 2007, **1**, (1), pp. 119–126
17 Bo, F., Xiaoquan, L., Peng, X., *et al.*: 'The research UL-P of loss of excitation protection for generator based on the artificial neural networks'. Asia Pacific Power and Energy Engineering Conf. (APPEEC 2009), 2009, pp. 1–4
18 Morais, A.P., Cardoso, G., Mariotto, L.: 'An innovative loss-of-excitation protection based on the fuzzy inference mechanism', *IEEE Trans. Power Deliv.*, 2010, **25**, (4), pp. 2197–2204
19 Bi, T., *et al*: 'Adaptive loss of field protection based on phasor measurements'. Power and Energy Society General Meeting, 2011, pp. 1–4
20 Seethalekshmi, K., Singh, S.N., Srivastava, S.C.: 'A classification approach using support vector machines to prevent distance relay maloperation under power swing and voltage instability', *IEEE Trans. Power Deliv.*, 2012, **27**, (3), pp. 1124–1133
21 IEEE Std. C37.102, IEEE Guide for AC Generator Protection, 2006
22 IEEE, Tutorial on the Protection of Synchronous Generators, Special Publication of the IEEE Power System Relaying Committee, 2nd edn., 2011
23 Mason, C.R.: 'The art and science of protective relaying' (General Electric Co., John Wiley and Sons, 1967)
24 Reimert, D.: 'Protective relaying for power generation systems' (CRC Press, 2006)
25 Duda, R.O., Hart, P.E., Stork, D.G.: 'Pattern classification' (John Wiley and Sons, 2001, 2nd edn.)
26 Canadian/American EMTP User Group, Alternative Transients Program Rule Book, 2002
27 Pajuelo, E., Gokaraju, R., Sachdev, M.S.: 'Loss of excitation protection for generators using a support vector machine technique'. Student Poster, IEEE Power Engineering Society General Meeting (PES-GM), Calgary, July 2009
28 IEEE Std. 421.5, IEEE Recommended Practice for Excitation System Models for Power System Stability Studies – 2005, April 2006

9 Appendix

9.1 Appendix: Generator data

MVA base: 104.4 MVA
Inertia constant: H 3.09 KW-sec/KVA
Synchronous: X_d 1.48 pu
Synchronous: X_q 1.42 pu
Transient: X'_d 0.193 pu
Transient: X'_q 0.484 pu
Subtransient: X''_d 0.136 pu
Subtransient: X''_q 0.132 pu
Leakage: Xl_m 0.14 pu
Transient: T_{do}' 3.59 s
Transient: T_{qo}' 0.312 s
Subtransient: T_{do}'' 0.033 s
Subtransient: T_{qo}'' 0.084 s

9.2 Appendix: Excitation system data

IEEE standard excitation system model-type ST1A [28]

K_A: 210
T_A: 0 s
T_C: 1.0 s
T_B: 1.0 s
T_{C1}: 0 s
T_{B1}: 0 s
$V_{R\mathrm{MAX}}$: 6.43 pu
$V_{R\mathrm{MIN}}$: −6.0 pu
K_C: 0.038
K_F: 0
T_F: 0 s
K_{LR}: 4.54
I_{LR}: 4.4 pu

IEEE standard power-system stabiliser PSS2A [28]

K_{S1}: 20
K_{S2}: 1.13
K_{S3}: 1
$T_1 = T_3$: 0.16 s
$T_2 = T_4$: 0.02 s
$T_{W1} = T_{W2} = T_{W3}$: 10 s
T_{W4}: 0 s
M: 2
N: 4
$V_{ST\mathrm{MAX}}$: 0.20 pu
$V_{ST\mathrm{MIN}}$: −0.066 pu
T_6: 0 s
T_7: 10 s

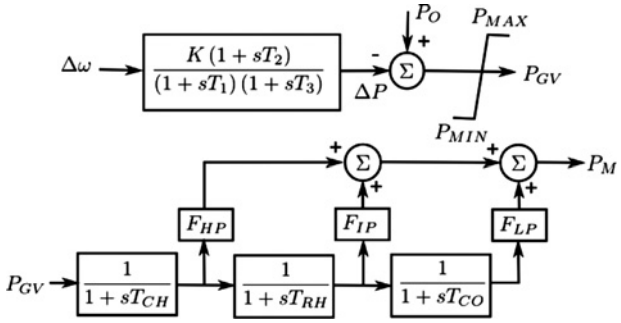

Fig. 8 *Governor model*

T_8: 0.3 s
T_9: 0.15 s

9.3 Appendix: Governor data Fig. 8

K: 18
T_2: 0 s
T_1: 0.077 s
T_3: 0.198 s
P_{MIN}: 0 pu
P_{MAX}: 0.95 pu
T_{CH}: 0.025 s
T_{RH}: 7 s
T_{CO}: 0.28 s
F_{HP}: 0.27
F_{IP}: 0.2555
F_{LP}: 0.4745

doi: 10.1049/iet-gtd.2012.0340